Electronic structure of Cu(100), Ag(100), Au(100), and $Cu_3Au(100)$ from inverse photoemission

F. J. Himpsel and J. E. Ortega
IBM Research Division, Thomas J. Watson Research Center,
P.O. Box 218, Yorktown Heights, New York 10598
(Received 20 April 1992)

Important parameters of the bulk and surface electronic structure are obtained for Cu(100), Ag(100), Au(100), and $Cu_3Au(100)$ surfaces using inverse photoemission with a high-resolution, tunable detector. The transitions from the Fermi level to the upper Δ_1 s,p band are found at 10.5, 9.6, 7.9, and 10.2 eV along the [100] direction, respectively. Their widths are about 1.3 eV. Upper limits for the X_4' points are found from the intensity cutoff above the band edge at 1.8, 1.9, 2.3, and 1.8 eV, with the best estimates for the X_4' positions at 1.8, 1.6, 1.6, and 1.8 eV. The $n=1$ image states are located at 4.1, 3.9, 4.75 (4.85), and 4.5 eV. A possible $n=0$ surface resonance is seen at 1.4, 1.3, 1.5, and 1.3 eV.

I. INTRODUCTION

This study establishes the electronic structure of noble-metal surfaces that are used as substrates for a variety of promising magnetic structures. For example, monolayers of transition metals on Ag(100) and Au(100) exhibit enhanced magnetic moments according to theoretical predictions,[1] and even some paramagnetic transition metals are expected to become ferromagnetic in monolayer form.[2] The metastable fcc phases of Fe and Co can be stabilized[3] on Cu(100), and by expanding the lattice constant from Cu to Cu_3Au a switch from a low-spin to a high-spin phase of fcc Fe has been observed.[4] Magnetic superlattices with noble-metal spacer layers exhibit oscillations between ferromagnetic and antiferromagnetic coupling that are most pronounced in the (100) orientation.[5] These oscillations are related to quantum-well states that show up in thin films of noble metals on the (100) surface of ferromagnets.[6,7]

II. SURFACE PREPARATION

In order to obtain optimum surface quality with soft materials, such as noble metals, we found it necessary to go through careful electrochemical polishing procedures that remove the damage done by mechanical polishing. For Cu we used an electropolishing method[8] based on an electrolyte of 40-ml phosphoric acid (85%), 9-ml water, and 5-ml sulphuric acid (98%) at about 30 C with a Cu cathode. The voltage was kept constant at 1.8 V, while the current decreased and eventually leveled out after a few minutes of polishing. For Ag(100) we alternated mechanical polishing cycles with chemical etching by a solution of 3 parts ammonium hydroxide and 1 part hydrogen peroxide (30%) for a few seconds. As a final chemical polish we applied a solution of 80-ml water, 10-ml saturated solution of CrO_3, and 4.5-ml dilute hydrochloric acid (9%) with a cotton swab, constantly wiping off the milky film that formed on the surface (Ref. 9). For Au(100) the cyanide-based recipe described by Tegart[8] was used. After polishing the surfaces were cleaned by sputter annealing with 0.5–1-keV Ar ions at angles of $\pm 30°$ from grazing and annealing temperatures in the 500 °C range. Cu(100) and Ag(100) gave bright 1×1 low-energy electron-diffraction patterns, Au(100) showed the 5×20 reconstruction, and $Cu_3Au(100)$ the structure of the ordered[10] alloy, which is equivalent to a $c(2\times2)$ pattern on a Cu(100) surface. By sputtering the Au(100) surface without annealing a somewhat disordered 1×1 structure was obtained, similar to the impurity-stabilized 1×1 structure reported previously.[11] The best indicators for surface quality turned out to be inverse photoemission features, such as the peak height of the $n=1$ image state and the depth of the emission minimum in the s,p gap.

III. BULK EMISSION

The band topology at the Cu(100), Ag(100), and Au(100) surfaces exhibits two branches of the Δ_1 s,p band for parallel momentum $k^{\parallel}=0$, which are separated by a large gap between the X_4' and X_1 points. The lower branch crosses the Fermi level at a wave vector k_F close to X, which is well-established from de Haas–van Alphen data.[12] For disordered $Cu_3Au(100)$ the same band topology would apply, but for the ordered alloy we have to consider extra reciprocal-lattice vectors that can transfer momentum. We find this umklapp effect weak enough to allow us interpreting all the major features by a simple fcc band structure without the extra lattice vectors. A key band-structure feature that can be determined[13] without assumptions about the upper band in photoemission and inverse photoemission is the transition energy between the lower and upper s,p branch at k_F. This Fermi-level crossing can be seen in Fig. 1 for Cu(100). To determine the exact transition energy and width we plot the emission intensity for states at the Fermi level E_F versus photon energy in Figs. 2(a)–2(d). For Cu(100) photoemission and inverse photoemission give an identical transition energy of 10.5 eV for states at E_F. In previously published photoemission data[13,14] a transition energy of 10.6 eV is quoted for states at $E_F-0.13$ eV, which is consistent with our results at E_F when taking the s,p-band dispersion into account. The widths are compara-

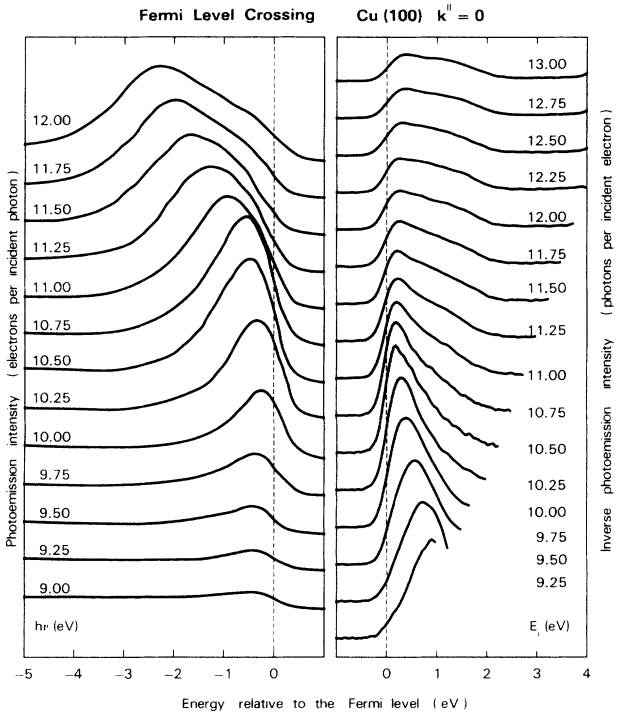

FIG. 1. Photoemission (Ref. 13) and inverse-photoemission spectra from Cu(100) showing the Δ_1 s,p-band crossing the Fermi level for parallel momentum $k^{\parallel}=0$. Vertical cuts at the Fermi level are given in Fig. 2(a).

ble in photoemission and inverse photoemission, with the main difference being that inverse photoemission exhibits a broader tail on the high-energy side. That is likely due to the wider $k^{\parallel}$ acceptance of the inverse-photoemission setup. A similar transition is seen for Ag(100) and $Cu_3Au(100)$ at 9.6 and 10.2 eV. For Au(100) the transition falls below the photon energies accessible to our inverse-photoemission setup, but can be seen in photoemission.[15] Although there is some uncertainty in the normalization of the photoemission data, one can see in Fig. 2(c) that the intensity at E_F peaks near 7.9 eV. In addition, there exists a second transition at 10.6 eV, which can be assigned to the next higher band, which has Δ_5 symmetry. This band has also been seen in photoemission.[15,16]

Comparing our data with first-principles, local-density band calculations[17] we find good agreement. The calculated Δ_1 transition energies at k_F of about 10.5, 8.6, and 8.1 eV are close to the experimental values of 10.5, 9.6, and 7.9 eV for Cu, Ag, and Au, respectively. The extra Δ_5 transition for Au at 10.6 eV fits to the lower branch of the calculated spin-orbit pair at about 10.9 eV. The upper branch calculated at 12.2 eV explains the transition found at 12 eV in Ref. 16. The good agreement for Au should settle a debate on whether or not local-density theory is 3–4 eV off for the s,p band of Au (see Ref. 16 and references therein). In Sec. IV we obtain upper limits of 1.8, 1.9, and 2.3 eV for the X_4' point of Cu, Ag, and Au, and best estimates of 1.8, 1.6, and 1.6 eV. These are to be compared to local-density values[17] of about 2.0, 2.1, and 1.6 eV. For a comparison with other band calculations of Cu, Ag, and Au see Ref. 17; for a band calculation of $Cu_3Au(100)$ see Ref. 19.

There exists a large database of photoemission and inverse-photoemission results from noble metals [for a review of photoemission data from Cu, Ag, and Au, see Ref. 17; for photoemission from $Cu_3Au(100)$, see Refs. 18 and 19; for inverse-photoemission results from Cu, Ag, and Au(100), see Refs. 20–34; for two-photon photoemission, see Refs. 35 and 36]. Previous data are consistent with our findings, except for the relative intensities of various features, which are affected by differences in the experimental geometry and energy resolution. Despite extensive prior inverse-photoemission work, we have obtained additional information by looking at $Cu_3Au(100)$, and by utilizing the tunability of our detector[37] to pin

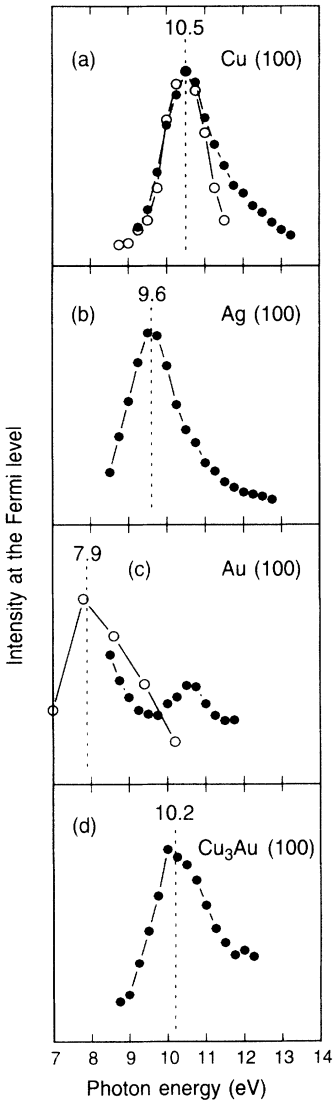

FIG. 2. (a)–(d) Fermi-level crossing of the Δ_1 s,p band in Cu(100), Ag(100), Au(100), and $Cu_3Au(100)$ at $k^{\parallel}=0$. The photoemission (Refs. 13–15) and inverse-photoemission intensity of states at the Fermi level is plotted vs photon energy (open and full circles, respectively). For Au(100) a secondary transition to the higher-lying Δ_5 band is seen at 10.6 eV.

down the transitions at the Fermi level. Thereby one is able to take advantage of the well-known Fermi wave vector for obtaining accurate, absolute band-structure points.

An unusual piece of information can be gathered from following a band closely as it disperses through the Fermi level and changes its character from occupied to unoccupied, such as in Fig. 1. In general, the transition from a positive ion final state in photoemission to a negative ion state in inverse photoemission does not have to be smooth. Coulomb energy can split positive and negative ion states for highly correlated bands. Of course, charge is well screened in a metal, and there is little doubt that noble metals behave as Fermi liquids, and do not exhibit a correlation gap. Nevertheless, the continuous band dispersion through the Fermi level in Fig. 1 and the coincidence of the Fermi-level crossings in photoemission and inverse photoemission in Fig. 2(a) place an upper bound of 0.05 eV on a residual Coulomb energy in the s,p band of Cu.

IV. SURFACE EMISSION

We can utilize the tunability of our detector[37] to avoid direct bulk transitions by working at energies higher than the Fermi-level crossing of the s,p band. This detection mode is very useful for isolating surface features and becoming sensitive to a monolayer of a magnetic material.[3,6] Inverse-photoemission spectra typical for this energy range are shown in Figs. 3(a)–3(d) for Cu(100), Ag(100), Au(100), and $Cu_3Au(100)$. They are independent of the incident electron energy, i.e., independent of the perpendicular momentum $k^{\perp}$, which provides evidence for the surface character of the whole spectrum. At energies of about 4 eV a large peak is seen for all three surfaces, which corresponds to the $n=1$ image-potential state. These are the most pronounced image states seen with inverse photoemission so far, due to our high resolution (<0.26 eV total[37]) and careful electrochemical surface preparation. It is even possible to discern the $n=2$ state as a weak feature above the $n=1$ peak. The $n=1$ energy positions of 4.1 and 3.9 eV for Cu(100) and Ag(100) and the $n=2$ peak at 4.55 eV for Cu(100) are close to the values of 4.06, 3.90, and 4.45 eV obtained from two-photon photoemission.[35,36] For Au(100) there is a small decrease in the $n=1$ image-state energy from 4.85 to 4.75 eV when going from the 1×1 to the 5×20 reconstruction.

The remaining emission within 2 eV of the Fermi level is due to transitions from evanescent initial states into the lower branch of the bulk Δ_1 s,p band. The intensity dropoff into the band gap above 2 eV marks the upper edge of the band at X_4'. However, this is only an upper limit, since there is a possible contribution from an $n=0$ surface resonance that is expected[25,27,29] in this energy range. Taking the inflection point as marker for this dropoff we obtain values that are consistent with independent results from the asymptotic energies of quantum-well states.[7] For Cu(100) the two different methods give the same X_4' point at 1.8 eV, while for Ag(100) and Au(100) 1×1 the intensity cutoff moves up to 1.9 and 2.3 eV, while the quantum-well value for X_4' moves down to 1.6 and 1.6 eV. At the same time the $n=0$ resonance becomes more and more pronounced, as it comes closer to the band edge. It creates extra emission in the gap that shifts the intensity dropoff up into the gap above X_4'. For the Au(100) 5×20 surface the $n=0$ feature is absent, probably due to the different surface structure, which consists of a close-packed, hexagonal overlayer. In this case the intensity dropoff into the gap is consistent with the X_4' position of 1.6 eV obtained from quantum-well states. For Cu_3Au our best estimate for the X_4' position equals that of Cu within our accuracy, using a linear interpolation between Cu and Au. This is corroborated by

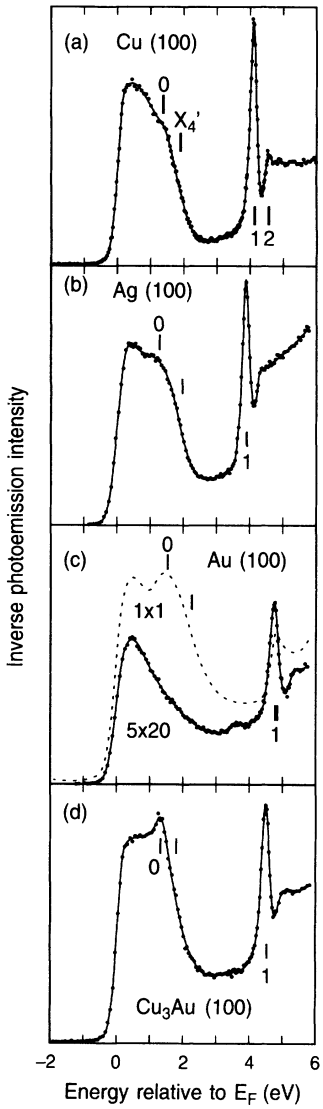

FIG. 3. (a)–(d) Inverse-photoemission spectra from Cu(100), Ag(100), Au(100), and $Cu_3Au(100)$ for $k^{\parallel}=0$ at an initial energy of 14.5 eV, where no direct bulk transitions are possible. The remaining surface emission shows a gap in the one-dimensional density of states above X_4', which contains a Rydberg series of $n=1,2,\ldots$ image states converging towards the vacuum level. A possible surface resonance corresponding to the $n=0$ extrapolation of this series shows up just below X_4'.

the interband transitions in Fig. 2, where Cu_3Au is much closer to Cu than to Au.

Several connections with other work on surface, image, and quantum-well states can be made from our data. For example, it turns out that the lowest quantum-well state[6] for Fe on Au(100) approaches the position of the $n=0$ resonance in the limit of coverage zero, where Fe is embedded as an impurity near the Au surface. A similar connection with an intrinsic surface state has been found for Ag on Fe(100), where an Ag-induced quantum-well state converges onto a surface state of Fe(100) in the zero coverage limit.[6,38] Another peculiar feature of the surface-sensitive spectra in Fig. 3 is a steplike intensity increase above the image state peaks. For Cu and Ag the step is too low in energy to be explained by the upper end of the s,p gap at X_1, which lies at 7.8 and 7.5 eV, respectively.[7] A more likely explanation is emission from states in the continuum of the image potential. Recent theoretical work[39–41] gives a more detailed description of this phenomenon.

ACKNOWLEDGMENTS

The authors would like to acknowledge F. Jona and D. M. Zehner for providing the $Cu_3Au(100)$ crystals.

[1]C. L. Fu, A. J. Freeman, and T. Oguchi, Phys. Rev. Lett. **54**, 2700 (1985); Roy Richter, J. G. Gay, and John R. Smith, *ibid* **54**, 2704 (1985); A. J. Freeman and C. L. Fu, J. Appl. Phys. **61**, 3358 (1987); S. Blügel, B. Drittler, R. Zeller, and P. H. Dedrichs, Appl. Phys. A **49**, 547 (1989).

[2]Ming J. Zhu, D. M. Bylander, and Leonard Kleinman, Phys. Rev. B **43**, 4007 (1991); Olle Eriksson, R. C. Albers, and A. M. Boring, Phys. Rev. Lett. **66**, 1350 (1991); S. Blügel, *ibid.* **68**, 851 (1992).

[3]For fcc Fe on Cu(100), see F. J. Himpsel, Phys. Rev. Lett. **67**, 2363 (1991), and references therein. For fcc Co on Cu(100), see C. M. Schneider, P. Schuster, M. Hammond, H. Ebert, J. Noffke, and J. Kirschner, J. Phys. Condens. Matter **3**, 4349 (1991); and G. J. Mankey, R. F. Willis, and F. J. Himpsel (unpublished).

[4]U. Gradmann and H. O. Isbert, J. Magn. Magn. Mater. **15-18**, 1109 (1980).

[5]S. S. P. Parkin, R. Bhadra, and K. P. Roche, Phys. Rev. Lett. **66**, 2152 (1991); J. J. de Miguel, A. Cebollada, J. M. Gallego, R. Miranda, J. Magn. Magn. Mater. **93**, 1 (1991); W. R. Bennett, W. Schwarzacher, and W. F. Egelhoff, Jr., Phys. Rev. Lett. **65**, 3169 (1990); W. F. Egelhoff, Jr. and M. T. Kief, Phys. Rev. B **45**, 7795 (1992); F. Petroff, A. Barthélemy, D. H. Mosca, D. K. Lottis, A. Fert, P. A. Schroeder, W. P. Pratt, Jr., R. Loloee, and S. Lequien, *ibid.* **44**, 5355 (1991); Z. Q. Qiu, J. Pearson, and S. D. Bader, *ibid.* (to be published).

[6]F. J. Himpsel, Phys. Rev. B **44**, 5966 (1991).

[7]J. E. Ortega and F. J. Himpsel, Phys. Rev. Lett. **69**, 844 (1992); J. E. Ortega, F. J. Himpsel, G. J. Mankey, and R. F. Willis (unpublished).

[8]W. J. Tegart, *The Electrolytic and Chemical Polishing of Metals in Research and Industry* (Pergamon, London, 1960), Chap. 7.

[9]H. J. Levinstein and W. H. Robinson, J. Appl. Phys. **33**, 3149 (1962). We followed closely a sequence described by P. Sanda, Ph.D. thesis, Cornell University (1992).

[10]V. S. Sundaram, B. Farrell, R. S. Alben, and W. D. Robertson, Phys. Rev. Lett. **31**, 1136 (1973).

[11]J. F. Wendelken and D. M. Zehner, Surf. Sci. **71**, 178 (1978); P. Heimann, J. Hermanson, and H. Miosga, Phys. Rev. Lett. **43**, 1757 (1979).

[12]P. T. Coleridge and I. M. Templeton, Phys. Rev. B **25**, 7818 (1982).

[13]D. E. Eastman, J. A. Knapp, and F. J. Himpsel, Phys. Rev. Lett. **41**, 825 (1978); J. A. Knapp, F. J. Himpsel, and D. E. Eastman, Phys. Rev. B **19**, 4952 (1979).

[14]The photoemission data for Cu(100) in Figs. 1 and 2 are taken from the same data set as the results published in Ref. 13. A background has been subtracted for the intensity curve in Ref. 13, while Fig. 2 plots the raw intensity.

[15]G. V. Hansson and S. A. Flodström, Phys. Rev. B **18**, 1572 (1978).

[16]R. Rosei, R. Lässer, N. V. Smith, and R. L. Benbow, Solid State Commun. **35**, 979 (1980).

[17]H. Eckardt, L. Fritsche, and J. Noffke, J. Phys. F **14**, 97 (1984).

[18]W. Eberhardt, S. C. Wu, R. Garrett, D. Sondericker, and F. Jona, Phys. Rev. B **31**, 8285 (1985).

[19]G. S. Sohal, C. Carbone, E. Kisker, S. Krummacher, A. Fattah, W. Uelhoff, R. C. Albers, and P. Weinberger, Z. Phys. B **78**, 295 (1990).

[20]V. Dose, W. Altmann, A. Goldmann, U. Kolac, and J. Rogozik, Phys. Rev. Lett. **52**, 1919 (1984).

[21]D. Straub and F. J. Himpsel, Phys. Rev. Lett. **52**, 1922 (1984).

[22]D. Straub and F. J. Himpsel, Phys. Rev. B **33**, 2256 (1986).

[23]W. Altmann, V. Dose, A. Goldmann, U. Kolac, and J. Rogozik, Phys. Rev. B **29**, 3015 (1984).

[24]V. Dose, U. Kolac, G. Borstel, and G. Thörner, Phys. Rev. B **29**, 7030 (1984).

[25]A. Goldmann, V. Dose, and G. Borstel, Phys. Rev. B **32**, 1971 (1985).

[26]W. Jacob, V. Dose, U. Kolac, Th. Fauster, and A. Goldmann, Z. Phys. B **53**, 459 (1986).

[27]R. Schneider, H. Dürr, Th. Fauster, and V. Dose (unpublished).

[28]Th. Fauster, R. Schneider, and H. Dürr (unpublished).

[29]D. P. Woodruff, S. L. Hulbert, P. D. Johnson, and N. V. Smith, Phys. Rev. B **31**, 4046 (1985).

[30]S. L. Hulbert, P. D. Johnson, N. G. Stoffel, W. A. Royer, and N. V. Smith, Phys. Rev. B **31**, 6815 (1985).

[31]S. L. Hulbert, P. D. Johnson, M. Weinert, and R. F. Garrett, Phys. Rev. B **33**, 760 (1986).

[32]C. Lang, T. Mandel, C. Laubschat, and G. Kaindl, J. Electron Spectrosc. Relat. Phenom. **52**, 49 (1990).

[33]B. Reihl, K. H. Frank, and R. R. Schlittler, Phys. Rev. B **30**, 7328 (1984).

[34]Bong-soo Kim, Sayong Hong, Rong Liu, and David W. Lynch, Phys. Rev. B **40**, 10 238 (1989).

[35]W. Steinmann, Appl. Phys. A **49**, 365 (1989).

[36]W. Schoenlein, J. G. Fujimoto, G. L. Eesley, and T. W. Capehart, Phys. Rev. B **43**, 4688 (1991).

[37]The experimental setup is described in Th. Fauster, D. Straub, J. J. Donelon, D. Grimm, A. Marx, and F. J. Himpsel, Rev.

Sci. Instrum. **56**, 1212 (1985); The energy resolution has been improved since then by lowering the cathode temperature and improving the accuracy of the position-sensitive detector [see F. J. Himpsel, Phys. Rev. B **43**, 13 394 (1991)].

[38]N. B. Brookes, Y. Chang, and P. D. Johnson, Phys. Rev. Lett. **67**, 354 (1991).

[39]W. L. Schaich, Phys. Rev. B **45**, 3744 (1992).

[40]M. Nekovee and J. E. Inglesfield (unpublished).

[41]Compare also other calculations for the cross section of image states: P. M. Echenique and J. B. Pendry, J. Phys. C **11**, 2065 (1978); W. L. Schaich and J. T. Lee, Phys. Rev. B **44**, 5973 (1991); A. G. Eguiluz, M. Heinrichsmeier, A. Fleszar, and W. Hanke, Phys. Rev. Lett. **68**, 1359 (1992).